11595

A New Nonhydrolytic Single-Precursor Approach to Surfactant-Capped Nanocrystals of Transition Metal Oxides

Jörg Rockenberger, Erik C. Scher, and A. Paul Alivisatos*

*Department of Chemistry, Box 101
University of California, Berkeley, Berkeley California 94720*

The advent of new methods to prepare semiconductor and metal nanocrystals, specifically the injection of molecular precursors into hot organic surfactants, has yielded markedly improved samples with good size control, narrow size distributions, and good crystallinity of individual and dispersable nanocrystals.[1−3] It is of considerable interest to apply these methods to the synthesis of transition metal oxide nanoparticles, which typically are prepared by methods involving water as solvent or reactant.[4−9] Using nonhydrolytic preparations of metal oxide nanocrystals at high temperature in organic surfactants, one can expect markedly different properties with respect to defect structure and surface composition. So far, there has been only one example of the solution-based nonhydrolytic synthesis of individual TiO_2 nanocrystals.[10] Metal oxide nanocrystals with nonhydroxylated surfaces may have significant advantages for applications in catalysis, ceramics, energy storage, magnetic data storage, sensors, ferrofluids, etc.

We report here first results of a new nonhydrolytic single-precursor approach to the synthesis of dispersable nanocrystals of transition metal oxides. Metal Cupferron complexes M^xCup_x (M: metal ion; Cup: *N*-nitrosophenylhydroxylamine, $C_6H_5N(NO)O^-$), with the metal ion coordinated via the oxygen atoms of the Cup ligand in a bidentate manner, proved to be promising as molecular precursors. Metal cupferronates are used in the precipitation or extraction of metal ions from aqueous solution, and are easily prepared for many metal elements.[11] In the following, we demonstrate that injecting solutions of metal Cupferron complexes in octylamine into long-chain amines at 250−300 °C yields nanocrystals of iron oxide, manganese oxide, and copper oxide. These nanocrystals range from 4 to 10 nm in diameter, are crystalline, and are dispersable in organic solvents. As Cupferron complexes are available for almost all metal elements, the use of this precursor might offer an interesting general approach to metal oxide nanocrystals.

The preparation of the metal Cupferron precursor is based on the precipitation of metal ions from aqueous solution at a specific pH with Cupferron, the ammonium salt of *N*-nitrosophenylhydroxylamine (details of the synthesis and characterization of the metal cupferronates M^xCup_x (M: Fe^{3+}, Cu^{2+}, Mn^{2+}) are provided as Supporting Information). In all three cases the elemental

analysis and the powder X-ray diffraction (XRD) patterns agreed well with single-crystal data.[12−14] In addition, FT-IR spectroscopy excluded the presence of excess Cupferron, water, or solvent molecules, and agreed well with results given in the literature.[15]

Dried powders of metal cupferronates show sharp decomposition temperatures of 180, 230, and 205 °C for $FeCup_3$, $MnCup_2$, and $CuCup_2$, respectively, when heated in a DTA/TGA apparatus under nitrogen. XRD of the respective decomposition products reveals that they consist of γ-Fe_2O_3, MnO, and Cu. The latter is a consequence of the reduction of CuO/Cu_2O by the reducing atmosphere given by the organic decomposition products of the Cupferron complex. This result proves that metal Cupferron complexes can indeed act as molecular precursors for transition metal oxides in the absence of O_2 and H_2O.

In the following, a typical synthesis yielding iron oxide nanocrystals with 6−7 nm particle diameters is described. To remove oxygen and water, 7 g of trioctylamine was heated to 100 °C for 1−1.5 h and repeatedly evacuated to 20 mTorr and purged with Ar. A solution of 0.3 M $FeCup_3$ in octylamine was treated the same way at 60 °C. The reaction was initiated by the rapid injection of 4 mL of $FeCup_3$ stock solution into the trioctylamine at 300 °C under vigorous magnetic stirring and an Ar atmosphere. A color change of the solution from colorless to dark-brown and the evolution of gas indicated the decomposition of the metal Cupferron complex. After the solution was heated for 30 min at 225 °C, the reaction was stopped and the solution was allowed to cool. At room temperature the flask contained nanocrystals of iron oxide, in both a dark-brown, clear liquid supernatant and a precipitate. The latter results from the high concentration of nanocrystals and their limited solubility in trioctylamine at low temperature. Adding 1−2 mL of organic solvents such as toluene, $CHCl_3$, etc. to this precipitate yielded clear, deep-brown dispersions of iron oxide nanocrystals which were stable for weeks at room temperature. By addition of a 3-fold volume excess of methanol, the iron oxide nanocrystals could be reprecipitated as a brown powder. Adding methanol to the supernatant of the reaction led to a brown precipitate, which could also be redispersed and reprecipitated by suitable solvents. For both fractions, dispersion and reprecipitation could be repeated several times.

Similar procedures were used in the synthesis of manganese oxide and copper oxide nanocrystals. In the case of manganese oxide, an orange precipitate was obtained after the reaction, which changed color to brown upon dispersion in toluene. In the case of $CuCup_2$, hexadecylamine was used as a surfactant to disperse the precipitated nanocrystalline copper oxide in toluene or $CHCl_3$. In addition, the reaction had to be stopped immediately after injection since the formation of metallic Cu instead of the copper oxide is favored at high temperatures under the strongly reducing conditions of the reaction.

Powder XRD reveals the nanocrystalline nature of the samples (Figure 1, left). The diffraction patterns were fitted with the program PowderCell[16] using structure data for γ-Fe_2O_3, Mn_3O_4, and Cu_2O as models.[17−19] Using the Debye−Scherrer equation,[20] a crystallite size was determined for every reflection, and all were averaged to give the mean values reported in Figure 1 (left). These

(1) Murray, C. B.; Norris, D. J.; Bawendi, M. G. *J. Am. Chem. Soc.* **1993**, *115*, 8706−8715.
(2) Peng, X.; Wickham, J.; Alivisatos, A. P. *J. Am. Chem. Soc.* **1998**, *120*, 5343−5344.
(3) Sun, S.; Murray, C. *J. Appl. Phys.* **1999**, *85*, 4325−4330.
(4) Charles, S. W.; Popplewell, J. *Ferromagnetic Materials*; Northholland Publishing Co.: Amsterdam, New York, Oxford, 1982; Vol. 2.
(5) Brinker, C. J.; Scherer, G. W. *Sol-Gel Science*; Academic Press: San Diego, 1990.
(6) Ziolo, R. F.; Giannelis, E. P.; Weinstein, B. A.; O'Horo, M. P.; Ganguly, B. N.; Mehrotra, V.; Russell, M. W.; Huffman, D. R. *Science* **1992**, *257*, 219−223.
(7) Matijevic, E. *Chem. Mater.* **1993**, *5*, 412.
(8) Moumen, N.; Pileni, M. P. *Chem. Mater.* **1996**, *8*, 1128.
(9) Ying, J. Y. Special Issue: Sol-Gel Derived Materials. In *Chem. Mater.* **1997**, *9*, 2247−2670.
(10) Trentler, T. J.; Denler, T. E.; Bertone, J. F.; Agrawal, A.; Colvin, V. L. *J. Am. Chem. Soc.* **1999**, *121*, 1613−1614.
(11) *Comprehensive coordination chemistry: the synthesis, reactions, properties & applications of coordination compounds*, 1st ed.; Pergamon Press: Oxford, England, 1987; Vol. 2, Chapter 15.9.2.

(12) Helm, D. v. d.; Merritt, L. L.; Degeilh, R.; MacGillavry, C. H. *Acta Crystallogr.* **1965**, *18*, 355−362.
(13) Elerman, Y.; Atakol, O.; Svoboda, I.; Geselle, M. *Acta Crystallogr. C* **1995**, *51*, 1520−1522.
(14) Tamaki, K.; Okabe, N. *Acta Crystallogr. C* **1996**, *52*, 1612−1614.
(15) Kellner, R.; Prokopowski, P. *Anal. Chim. Acta* **1976**, *86*, 175−184.
(16) Nolze, G.; Kraus, W. *Powder Diffr.* **1998**, *13*, 256−259.
(17) Shmakov, A. N.; Kryukova, G. N.; Tsybulya, S. V.; Chuvilin, A. L.; Solovyeva, L. P. *J. Appl. Crystallogr.* **1995**, *28*, 141.
(18) Jarosch, D. *Mineral. Petrol.* **1987**, *37*, 15−23.
(19) Neuburger, M. C. *Z. Phys.* **1930**, *67*, 845−850.
(20) Cullity, B. D. *Elements of X-ray Diffraction*, 2nd ed.; Addison-Wesley: Reading, MA, 1978.
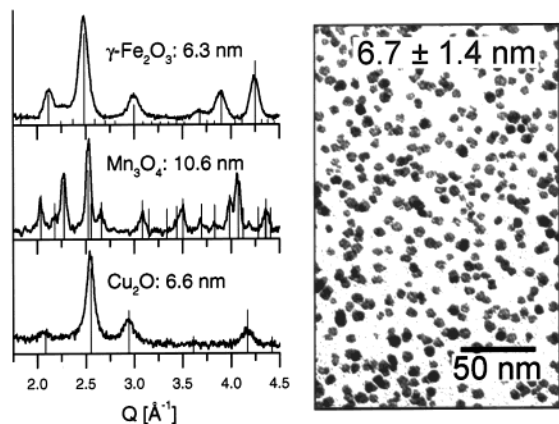
11596   *J. Am. Chem. Soc., Vol. 121, No. 49, 1999*

Communications to the Editor

Figure 1. XRD patterns of γ-Fe$_2$O$_3$, Mn$_3$O$_4$, and Cu$_2$O nanocrystals and expected lattice reflections of the respective bulk phases (left). A low-resolution TEM image of the corresponding sample of γ-Fe$_2$O$_3$ nanocrystals is shown at the right.

averaged crystallite sizes are in good agreement with mean diameters determined from low-resolution TEM imaging. The corresponding TEM image of the γ-Fe$_2$O$_3$ nanocrystals is shown in Figure 1 (right). The nanocrystals are individual and their average diameter is 6.7 nm with a standard deviation of 1.4 nm.

Particles with average sizes down to 4 nm were synthesized by lowering the injection temperature and/or lowering the injected precursor concentration. For instance, injecting the FeCup$_3$ precursor solution at 250 °C and refluxing at 200 °C for 30 min, instead of 300 and 225 °C as in the sample of Figure 1, yields γ-Fe$_2$O$_3$ nanocrystals 5.2 ± 1.5 nm in size. However, the injection of an additional 2 mL of precursor solution after 5 min of refluxing at 200 °C results in particles with diameters of 6.1 ± 1.8 nm. In all cases it was observed that subsequent extractions of the reaction precipitate with toluene yielded fractions containing continuously bigger particles. In the case of the preparation with an additional secondary injection, each subsequent extraction of the reaction precipitate resulted in approximately a 1 nm increase in the average particle diameter. Consequently, the fifth fraction contained γ-Fe$_2$O$_3$ nanocrystals which were 10.0 ± 1.5 nm in diameter. A low-resolution TEM image of this fraction is shown in Figure 2. Apparently, the slow evaporation of a dispersion of nanocrystals in toluene on a TEM grid leads to the formation of an extended monolayer of particles. The covered area is larger than 2 μm^2 and extends beyond the part shown in Figure 2. Each particle is separated from neighboring particles by its shell of surfactant. Currently, the relatively broad size distribution of 15% prevents the formation of ordered superlattices as observed with other systems.[3,21,22] However, we believe that by using size-selective precipitation[1,23] in addition to size-selective extraction during the isolation process, we will be able to achieve size distributions with less than 10% standard deviation.

The crystallinity of these particles is revealed by high-resolution TEM imaging as shown in Figure 2 (top left). The observed lattice plane distances of 4.77 and 4.11 Å, as well as the angle of about 50° between the crossed fringes, indicate the presence of tetragonal γ-Fe$_2$O$_3$ with an ordered superlattice of cation vacancies.[17] The corresponding lattice planes are (113) and (201), respectively, and the FFT (top right) of the high-resolution image indicates that the particle was imaged along its [51$\bar{2}$] zone axis. Neither cubic γ-Fe$_2$O$_3$ with a statistical distribution of cation vacancies over the octahedral sites nor Fe$_3$O$_4$ shows a similar agreement.[17,24] In other high-resolution TEM images, we observe
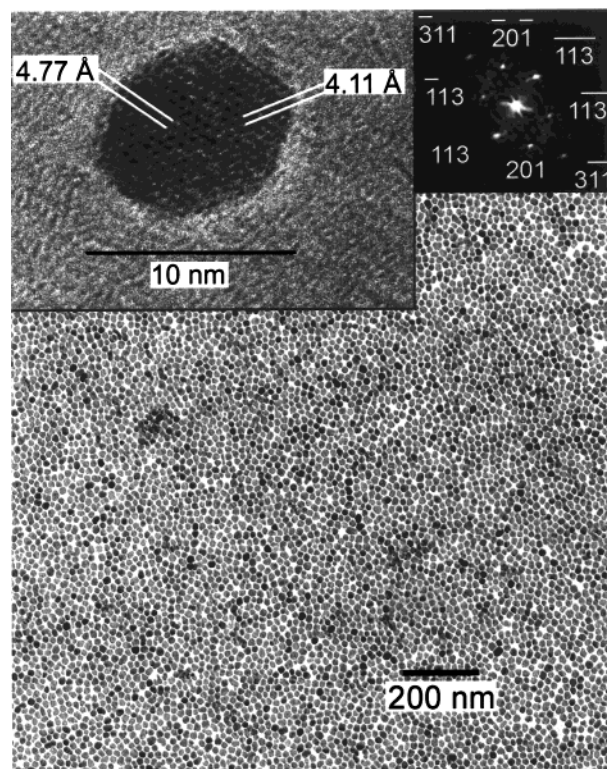

Figure 2. Low-resolution TEM image of a monolayer of individual γ-Fe$_2$O$_3$ nanocrystals (10.0 ± 1.5 nm) covering an area bigger than 2 μm^2. Top left: High-resolution TEM image of one of the nanocrystals in this sample. The indicated lattice plane distances correspond to the (113) and (201) lattice planes of tetragonal γ-Fe$_2$O$_3$ with ordered superlattice of the cation vacancies. Top right: FFT of the high-resolution TEM image looking down the [51$\bar{2}$] zone-axis.

particles with lattice plane distances of 4.97 and 4.27 Å that also belong uniquely to the tetragonal superstructure phase of γ-Fe$_2$O$_3$ (see table in Supporting Information). Interestingly, it has been reported that this ordered superstructure phase occurs only in particles with diameters larger than 100 nm.[25] To address this issue further, Mössbauer spectroscopy studies of our samples are currently in progress.

We have shown that it is possible to prepare dispersable nanocrystals of transition metal oxides in the absence of water or air by thermal decomposition of metal Cupferron complexes in hot surfactants. Preliminary experiments suggest that a similar level of size control as in the synthesis of semiconductor nanocrystals is possible. Since the precursor is available for many metal elements, this approach may present a rather general route to metal oxide nanocrystals.

Supporting Information Available: Description of the synthesis of metal cupferronates and their characterization by powder XRD, elemental analysis, FT-IR spectroscopy, and DTA/TGA measurements; low-resolution TEM images and size histograms of metal oxide nanocrystals; a table with lattice plane distances observed in high-resolution TEM imaging (PDF). This material is available free of charge via the Internet at http://pubs.acs.org.

JA993280V

(21) Bentzon, M. D.; Wonterghem, J. v.; Morup, S.; Tholen, A.; Koch, C. J. W. *Philos. Mag. B* **1989**, *60*, 169−178.

(22) Murray, C. B.; Kagan, C. R.; Bawendi, M. G. *Science* **1995**, *270*, 1335−1338.

(23) Chemseddine, A.; Weller, H. *Ber. Bunsen-Ges. Phys. Chem.* **1993**, *97*, 636−637.

(24) Fleet, M. E. *Acta Crystallogr. B* **1981**, *37*, 917−920.

(25) Cornell, R. M.; Schwertmann, U. *The Iron Oxides−Structure, Properties, Reactions, Occurrence and Uses*, 1st ed.; VCH Verlagsgesellschaft: Weinheim, Germany, 1996.